Supporting Information

Phosphorus doping of nickel-cobalt boride to produce a metal–metalloid–nonmetal electrocatalyst for improved overall water splitting

Amarnath T. Sivagurunathan[1], *Selvaraj Seenivasan*[1], *T. Kavinkumar*[1, 2], *and Do-Heyoung Kim*[1]*

[1]School of Chemical Engineering, Chonnam National University, 77 Yongbong-ro, Gwangju 61186, Republic of Korea.

[2]Centre for Energy and Environment, Department of Physics, Karpagam Academy of Higher Education, Coimbatore 641021, India.

*Corresponding author's email: kdhh@chonnam.ac.kr

Tel. (office): +82-62-530-1894

Experimental Section

Synthesis of nickel-cobalt oxide (NC)

518 mg of $CoCl_2.6H_2O$, 475 mg of $NiCl_2.6H_2O$, and 540 mg of NH_2CONH_2 were dissolved in a beaker containing 40 mL of deionized (DI) and stirred for 0.5 h. This solution was then transferred into a 50-mL Teflon autoclave. NF was cleaned using ethanol and DI water three times alternatively and then dried in an oven at 60 °C to remove the surface oxides. The NF was then transferred into the as-prepared solution and hydrothermal process was carried out at 120 °C and for 10 h. The obtained $NiCo_2O_4$ (NC) was rinsed with DI water and ethanol and then kept in oven at 60 °C for further use.

Synthesis of nickel-cobalt boride (NCB)

100 mg of $NaBH_4$ was dissolved in a beaker containing 40 ml of DI water and stirred for 5 min. A piece of NF coated with NC was placed into the reaction mixture, transferred into a 50-mL Teflon-lined autoclave. The hydrothermal reaction was carried out at 120°C for 180 min. The product was then washed with DI water and ethanol and kept in oven at 80°C for 8 h. The nickel cobalt boride (NCB) was then attained by annealing the material grown NF placed inside the tube furnace under nitrogen atmosphere at 350 °C for 0.5 h with a ramping rate of 2° min^{-1}.

Synthesis of phosphorus-doped nickel-cobalt oxide (P-NC)

Phosphorus-doped nickel cobalt oxide (P-NC) was synthesized to determine the effect of P doping in the absence of B. The P source $NaPH_2O_2$ was placed in a small crucible and the NC coated NF was placed over the boat in downstream nitrogen flowing inside tube furnace. $NiCo_2O_4$ was doped with 140 mg of P source under nitrogen atmosphere at 350 °C for 30 min (2° min^{-1}).

Characterizations

X-ray diffraction (XRD) analysis was analyzed using a Rigaku X-ray diffractometer with CuKα radiation. The morphology and microstructure of the samples were examined using high-resolution scanning electron microscopy (HR-SEM; JEOL JSM-7500F) and transmission electron microscopy (TEM; TECNAI G2 F20 TEM system). X-ray photoelectron spectroscopy (XPS) was done using an ESCALAB-MKII system (VG Scientific Co.). XPS had an Al K alpha source, and the results had been characterized by the Fityk software. Gaussian as a fitting function was used to characterize the XPS results.

Water-splitting measurements

The electrocatalytic performance of the as-prepared samples on NF was determined using a three-electrode cell in which a saturated calomel electrode (SCE) and Pt foil were employed as the reference and counter electrodes, respectively, for the OER, while an SCE and graphite rod were used as the reference and counter electrodes, respectively, for the HER. Data were acquired using an electrochemical workstation (WonATech WBCS30000). Linear sweep voltammetry (LSV) measurements were conducted at 2 mV s^{-1} for the OER and HER in 1 M KOH. Electrochemical impedance spectroscopy (EIS) measurements were taken using a Parstat 3000 workstation (0.01 Hz to 100 kHz with a 10-mV amplitude). Gas chromatography (074-594-P1E Micro GC Fusion, INFICON) was used to determine the amount of gaseous products. All of the potentials were calibrated to the reversible hydrogen electrode (RHE) using Eq. (9), while η was obtained using Eq. (10), and the Tafel slope was calculated using Eq. (11):

$$\mathbf{E_{RHE} = E_{SCE} + 0.059pH + 0.247} \quad \text{----------(9)}$$

$$\boldsymbol{\eta = E_{RHE} - 1.23} \quad \text{----------(10)}$$

$$\boldsymbol{\eta = b \log j + a} \quad \text{----------(11)}$$

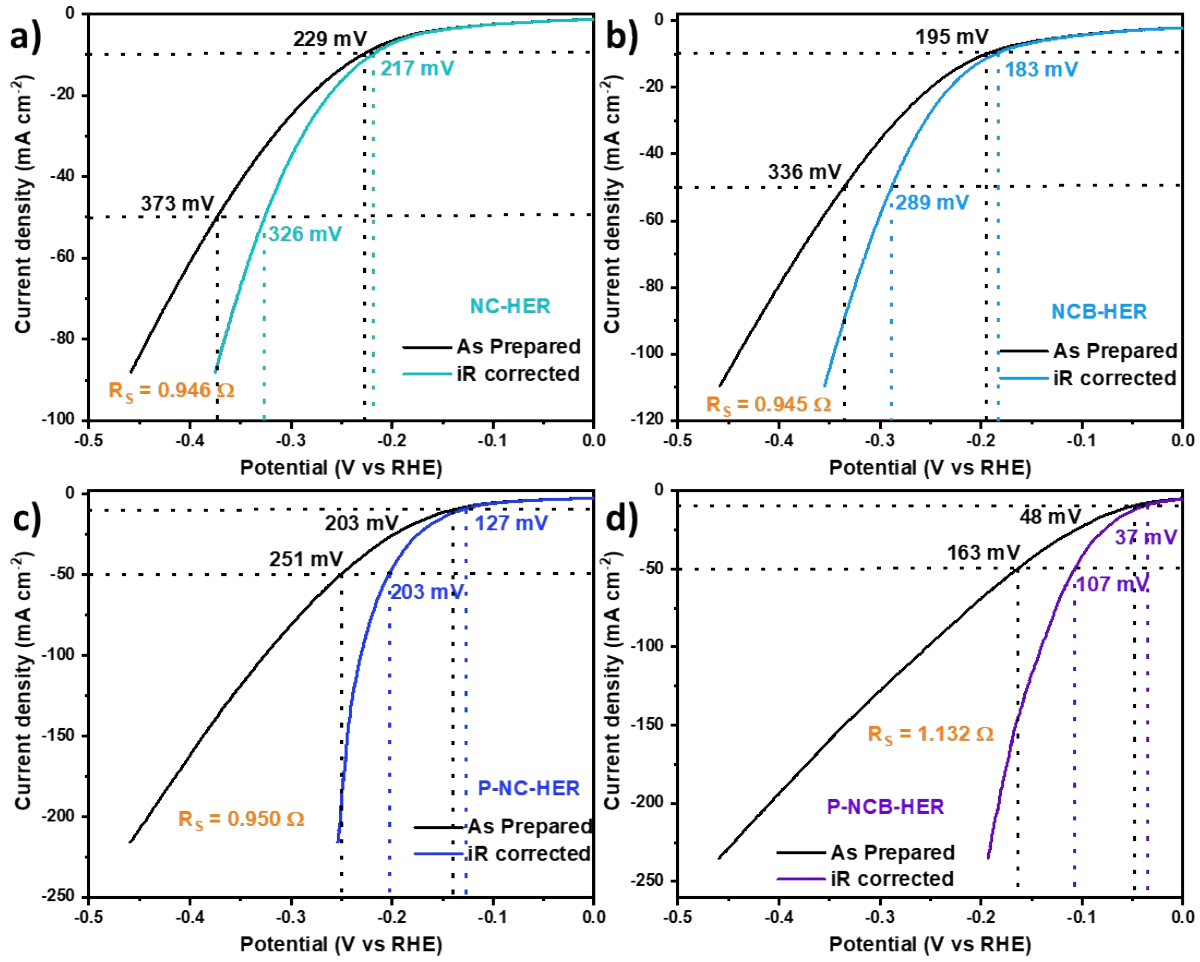

Fig. S1. HER half-cell LSV curves with and without iR compensation (a) NC, (b) NCB, (c) P-NC, and (d) P-NCB electrode.

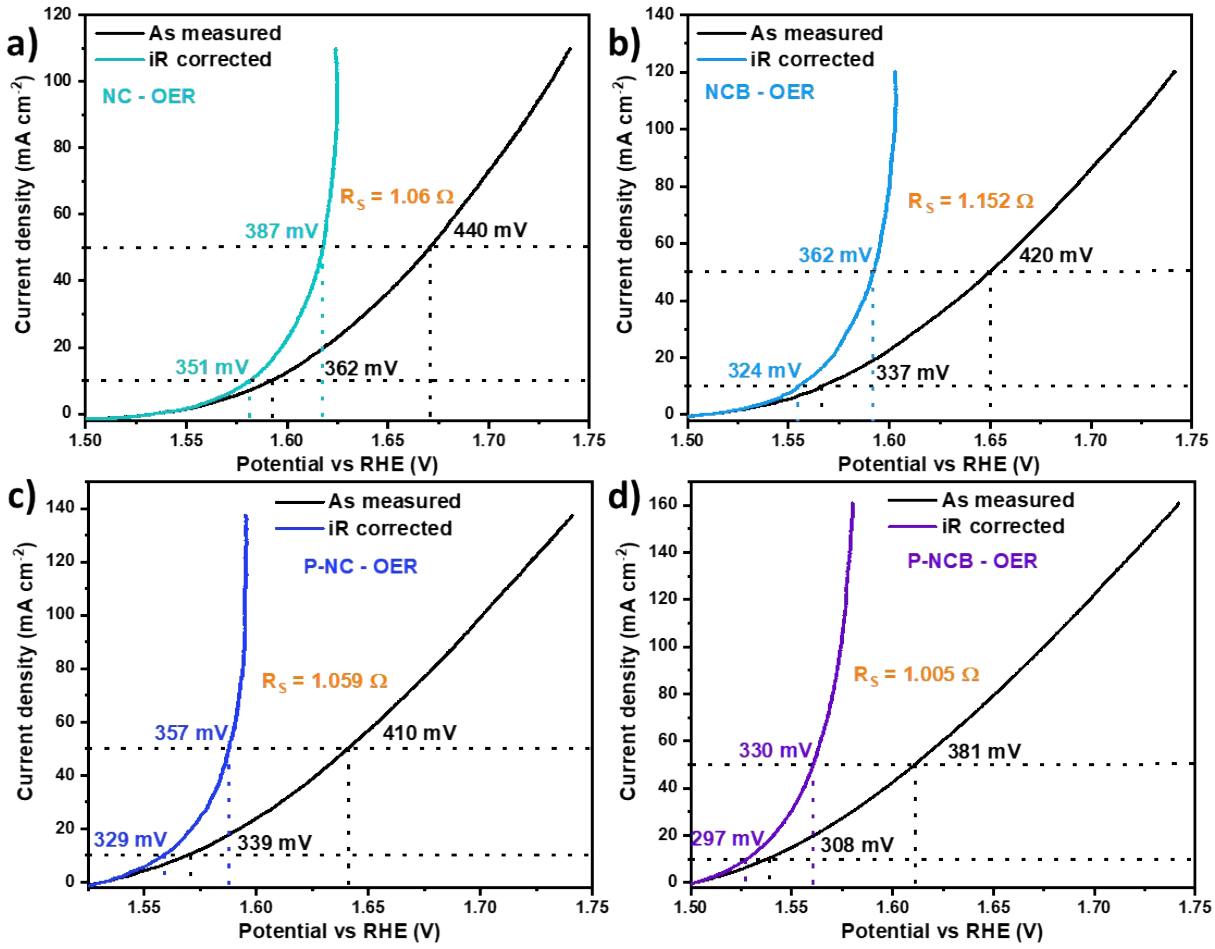

Fig. S2. OER half-cell LSV curves with and without iR compensation (a) NC, (b) NCB, (c) P-NC, and (d) P-NCB electrodes.

Table S1. Fitted data of electrochemical impedance spectra data shown in Fig. (a) As-prepared HER electrodes at –1.1 $V_{SCE,}$ (b) As-prepared OER electrodes at 0.4 $V_{SCE.}$

a)

Sample	R_s (Ω cm^{-2})	R_{ct} (Ω cm^{-2})
NC	0.9460	3.622
NCB	0.9459	1.472
P-NC	0.9507	1.59
P-NCB	1.132	1.315

b)

Sample	R_s (Ω cm^{-2})	R_{ct} (Ω cm^{-2})
NC	1.06	102.4
NCB	1.152	1.676
P-NC	1.059	2.232
P-NCB	1.005	0.706

Calculation of number of surface-active sites (N_A)

Associated charge with the reduction peak (Q) can be calculated using the following expression:

$$Q = \frac{\int I\, dV}{v}$$

where Q (C) is the total charge associated with the reduction peak and v (V/s) is the scan rate. For simplicity, we assume that all the surface redox reactions are single electron transfer reactions. Then, the number of electrons calculated above is the number of surface-active sites (N). q = 1.602 × 10^{-19} C.

$$N = \frac{Q}{q}$$

Electrochemical active surface area (ECSA) calculation

The electrochemical active surface area, which can be determined from the following formula:

$$\text{ECSA} = (specific\ capacitance\ /\ 40\ \mu F\ cm^{-2}\ )\ cm^2$$

Where C_{dl} represents the specific capacitance, and 40 μF cm-2 is a constant to convert capacitance to ECSA. The specific capacitance can be converted into an electrochemical active surface area (ECSA) using the specific capacitance value for a flat standard with 1.0 cm^2 of real surface area.

Turnover frequency calculation

TOF is the number of times of reaction per unit time and unit active site. Since the exact specific ratio of our hybrid catalyst is unknown, the molar weight cannot be calculated exactly. So we calculated the number of electrons consumed in the electrode reaction in order to find the number of surface active sites. To calculate the per-site turnover frequency (TOF), we used the following formula according to previous reports.

$$TOF\ per\ site = \frac{Total\ Hydrogen\ Turn\ Overs/cm^2 geometric\ area}{No.\ of\ Surface\ active\ sites\ /cm^2\ geometric\ area}$$

The number of total hydrogen turn overs is calculated from the current density using the following equation:

$$\#_{H_2} = \left(j\frac{mA}{cm^2}\right)\left(\frac{1C\ s^{-1}}{1000\ mA}\right)\left(\frac{1\ mol\ e^-}{96485.3\ C}\right)\left(\frac{1\ mol\ H_2}{2\ mol\ e^-}\right)\left(\frac{6.022\ \times 10^{23}\ H_2\ molecul}{1\ mol\ H_2}\right.$$
$$\left.\frac{H_2/s}{cm^2}\ per\ \frac{mA}{cm^2}\right)$$

The number of total oxygen turn overs is calculated from the current density using the following equation:

$$\#_{O_2}$$

$$= \left(j\frac{mA}{cm^2}\right)\left(\frac{1C\ s^{-1}}{1000\ mA}\right)\left(\frac{1\ mol\ e^-}{96485.3\ C}\right)\left(\frac{1\ mol\ O_2}{4\ mol\ e^-}\right)\left(\frac{6.022\ \times 10^{23}\ O_2\ molecul}{1\ mol\ O_2}\right.$$

$$\frac{H_2/s}{cm^2}\ per\ \frac{mA}{cm^2}$$

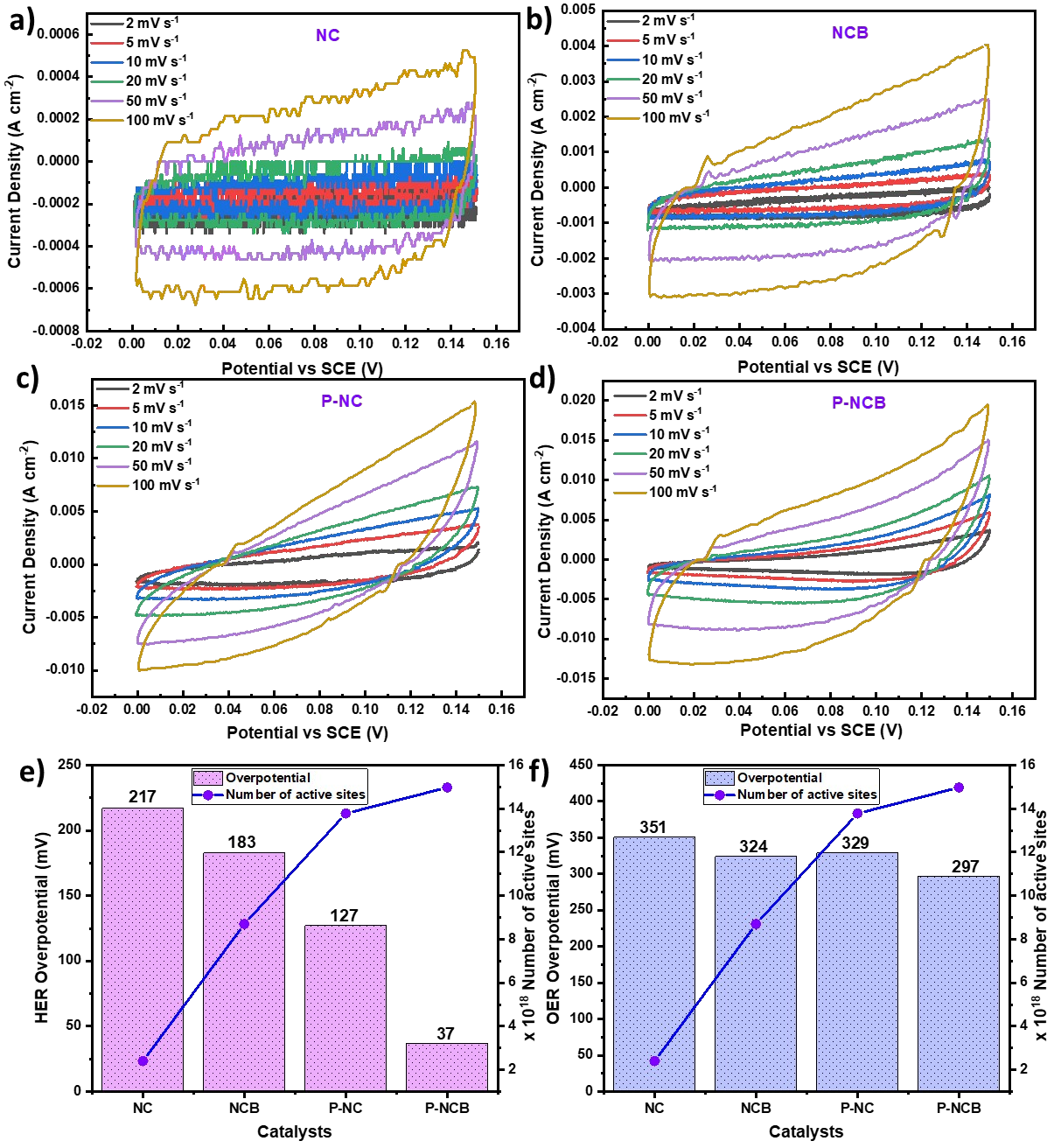

Fig. S3. CV profile of non-faradaic regions of (a) NC, (b) NCB, (c) P-NC, (d) P-NCB electrodes respectively, (e) HER overpotential at 10 mA cm^{-2} for the tested electrodes in comparison with N_A, and (f) OER overpotential at 10 mA cm^{-2} for the tested electrodes in comparison with N_A.

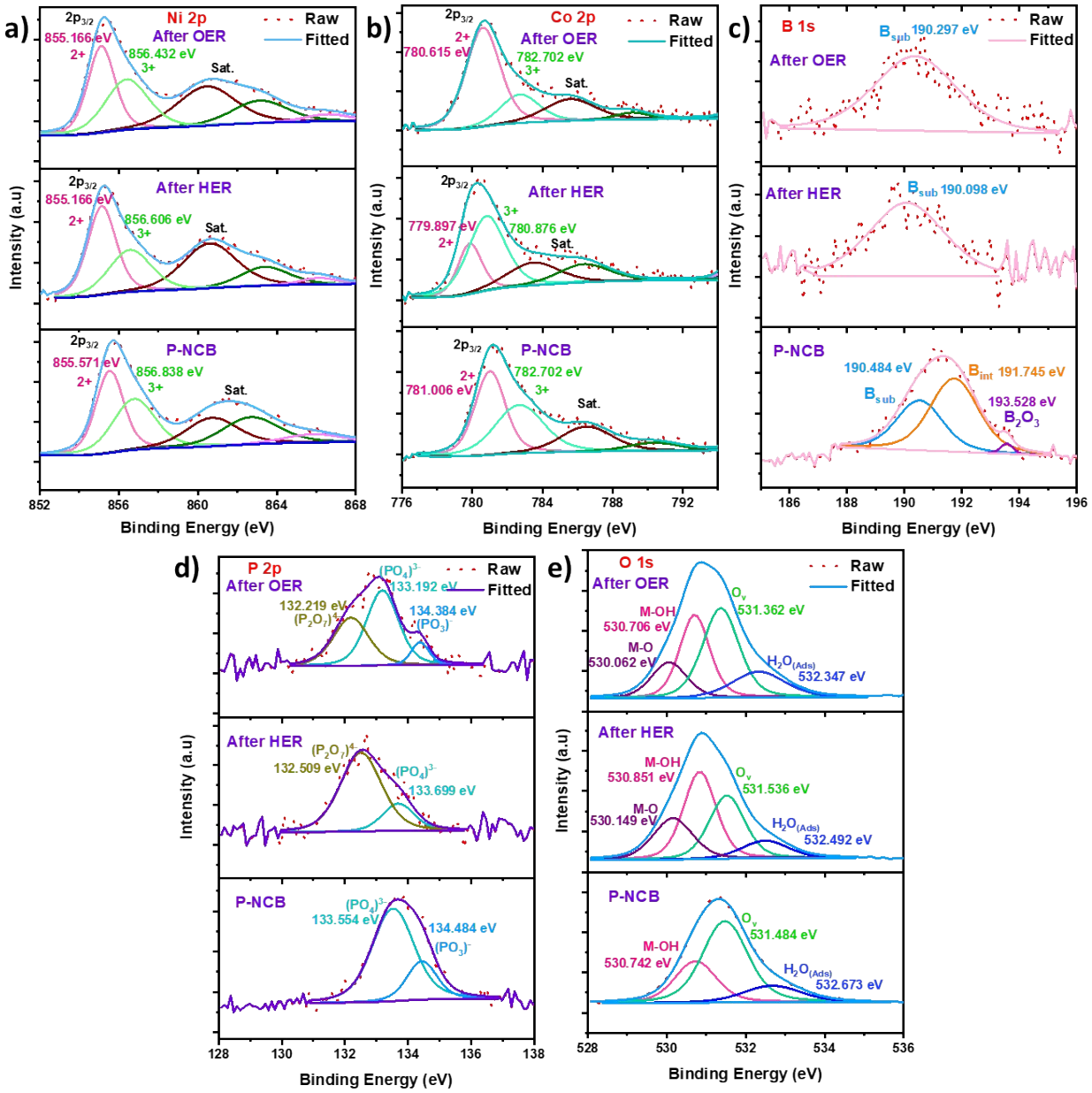

Fig. S4. XPS spectra After OER and HER of P-NCB nanostructure: (a) Ni 2p, (b) Co 2p, (c) B 1s, (d) P 2p, and (e) O 1s.

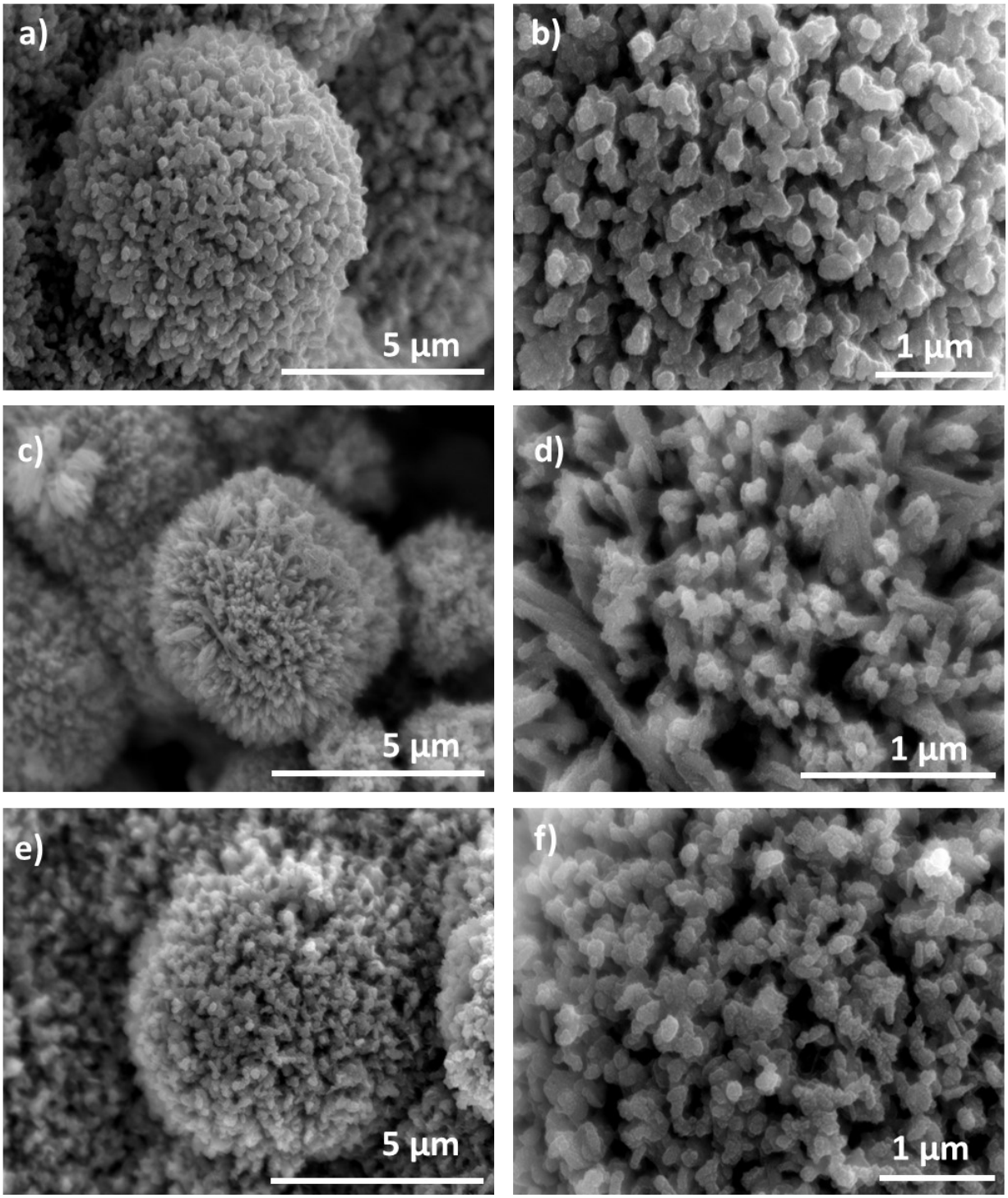

Fig. S5. HR-SEM images of P-NCB electrode (a, b) Before stability, (c, d) After HER stability, and (e, f) After OER stability.

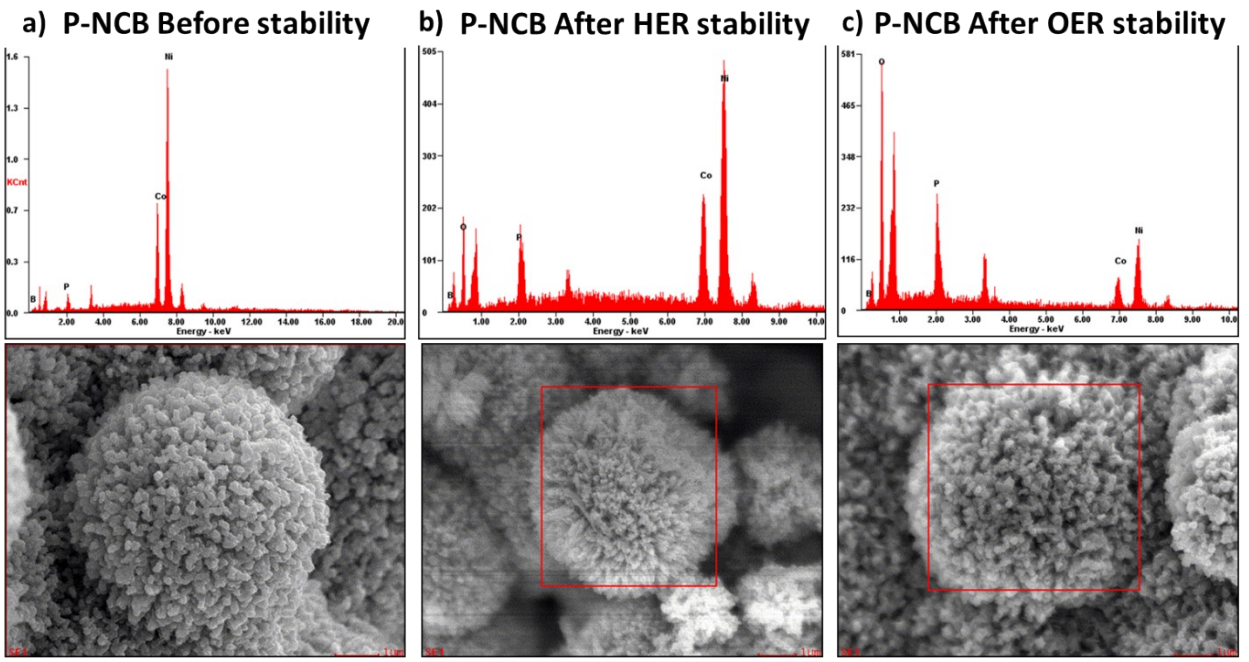

Element	Wt%	At%
BK	09.59	36.32
PK	01.06	01.40
CoK	22.98	15.97
NiK	66.37	46.30
Matrix	Correction	ZAF

Element	Wt%	At%
BK	08.98	32.83
OK	02.59	06.40
PK	02.10	02.68
CoK	22.97	15.41
NiK	63.37	42.68

Element	Wt%	At%
BK	12.48	32.11
OK	18.51	32.18
PK	07.21	06.48
CoK	17.11	08.08
NiK	44.68	21.16

Fig. S6. EDAX analysis on elemental composition of P-NCB electrode (a,) Before stability, (b) After HER stability, and (c) After OER stability.

Table S2. Comparison of the electrocatalytic activity of P-NCB for the HER in 1 M KOH with previously reported HER catalysts.

Catalyst	Electrolyte	Overpotential at 10 mA cm^{-2} (mV)	Tafel slope (mV dec^{-1})	Ref.
P-NCB (iR-compensated)	**1 M KOH**	**37@10 mA cm^{-2} 107@50 mA cm^{-2} 140@100 mA cm^{-2}**	**96**	**This work**
Annealed Co–Ni–B@NF	1 M KOH	205	-	1
Ni-Fe-P-B	1 M KOH	220	63	2
Ni-Fe-P@NC/NF	1 M KOH	66	81	3
CoP@NF	1 M KOH	195	175	4
Ni_xB/f-MWCNT	1 M KOH	116	70.4	5
CoP@NCHNCs	1 M KOH	93	67	6
Fe-CoNiP	1 M KOH	110	90.6	7
Co−B−P	1 M KOH	51	44	8
Ni–P	1 M KOH	52	37.4	9
Co-P	1 M KOH	136	56.2	10
$Ni_xFe_{1-x}B$	1 M KOH	63.5	56.3	11
NPO/NS-C	1 M KOH	88	65	12

Table S3. Comparison of the electrocatalytic activity of P-NCB for the OER in 1 M KOH with previously reported OER catalysts.

Catalyst	Electrolyte	Overpotential at 10 mA cm^{-2} (mV)	Tafel slope (mV dec^{-1})	Ref.
P-NCB (iR-compensated)	**1 M KOH**	**297@10 mA cm^{-2} 330@50 mA cm^{-2} 344@100 mA cm^{-2}**	**48.2**	**This work**
Annealed Co–Ni–B@NF	1 M KOH	313	120	1
BPO-Ni	1 M KOH	370	90	13
Ni-Fe-P-B	1 M KOH	269	38	2
Ni-B_i@NB	1 M KOH	302	52	14
CoP@NF	1 M KOH	317@50	64	15
CoP@NCHNCs	1 M KOH	304	93	6
Ni_2P	1 M KOH	290	-	16
Ni–P	1 M KOH	286	44	9
Co-P	1 M KOH	345	47	10

Table S4. Comparison of the electrocatalytic activity of P-NCB in a two-electrode configuration with 1 M KOH with previously reported catalysts.

Catalyst	Electrolyte	Voltage (V)	Ref.
P-NCB//P-NCB (iR-uncompensated)	**1 M KOH**	**1.605 V @ 10 mA cm^{-2} 1.802 V @ 50 mA cm^{-2} 1.954 V @ 100 mA cm^{-2}**	**This work**
Annealed Co–Ni–B@NF	1 M KOH	1.72 V @ 10 mA cm^{-2}	1
Ni-Fe-P-B over CFP	1 M KOH	1.62 V @ 10 mA cm^{-2}	2
Ni–P	1 M KOH	1.6 V @ 10 mA cm^{-2}	9
CoP@NF and CoP/CoO@NF	1 M KOH	1.62 V @ 10 mA cm^{-2}	17
CoP@NCHNCs	1 M KOH	1.62 V @ 10 mA cm^{-2}	6
Fe-CoNiP	1 M KOH	1.62 V @ 10 mA cm^{-2}	7
Ni_xB/f-MWCNT	1 M KOH	1.60 V @ 10 mA cm^{-2}	5
NPO/NS-C	1 M KOH	1.63 V @ 10 mA cm^{-2}	12
$CoxPO_4$/CoP	1 M KOH	1.91 V @ 10 mA cm^{-2}	18
Co_9S_8-$CoSe_2$	1 M KOH	1.66 V @ 10 mA cm^{-2}	19
MoP@Ni_3P/NF	1 M KOH	1.67 V @ 10 mA cm^{-2}	20

References

1. N. Xu, G. Cao, Z. Chen, Q. Kang, H. Dai and P. Wang, *J. Mater. Chem. A*, 2017, **5**, 12379-12384.
2. W. Tang, X. Liu, Y. Li, Y. Pu, Y. Lu, Z. Song, Q. Wang, R. Yu and J. Shui, *Nano Res.*, 2020, **13**, 447-454.
3. Y. Wang, S. Zhao, Y. Zhu, R. Qiu, T. Gengenbach, Y. Liu, L. Zu, H. Mao, H. Wang, J. Tang, D. Zhao and C. Selomulya, *iScience*, 2020, **23**, 100761-100761.
4. D. Liang, L. Zhang, W. He, C. Li, J. Liu, S. Liu, H.-S. Lee and Y. Feng, *Appl. Energy*, 2020, **264**, 114700.
5. X. Chen, Z. Yu, L. Wei, Z. Zhou, S. Zhai, J. Chen, Y. Wang, Q. Huang, H. E. Karahan, X. Liao and Y. Chen, *J. Mater. Chem. A*, 2019, **7**, 764-774.
6. Y. Chen, M. Wang, S. Xiang, J. Liu, S. Feng, C. Wang, N. Zhang, T. Feng, M. Yang, K. Zhang and B. Yang, *ACS Sustain. Chem. Eng.*, 2019, **7**, 10912-10919.
7. M. Ramadoss, Y. Chen, X. Chen, Z. Su, M. Karpuraranjith, D. Yang, M. A. Pandit and K. Muralidharan, *J. Phys. Chem. C*, 2021, **125**, 20972-20979.
8. X. Bao, Y. Li, J. Wang and Q. Zhong, *ChemCatChem*, 2020, **12**, 6259-6264.
9. D. Song, D. Hong, Y. Kwon, H. Kim, J. Shin, H. M. Lee and E. Cho, *J. Mater. Chem. A*, 2020, **8**, 12069-12079.
10. S. Adhikari, S. Selvaraj, S.-H. Ji and D.-H. Kim, *Small*, 2020, **16**, 2005414.
11. W. Hong, S. Sun, Y. Kong, Y. Hu and G. Chen, *J. Mater. Chem. A*, 2020, **8**, 7360-7367.
12. J. Tong, W. Li, L. Bo, Y. Li, T. Li and Q. Zhang, *Electrochim. Acta*, 2019, **320**, 134579.
13. X. Liu, J. Wu and X. Guo, *Electrochem. commun.*, 2020, **111**, 106649.

14. W.-J. Jiang, S. Niu, T. Tang, Q.-H. Zhang, X.-Z. Liu, Y. Zhang, Y.-Y. Chen, J.-H. Li, L. Gu, L.-J. Wan and J.-S. Hu, *Angew. Chem. Int. Ed.*, 2017, **56**, 6572-6577.

15. J. Liu, Y. Gao, X. Tang, K. Zhan, B. Zhao, B. Y. Xia and Y. Yan, *J. Mater. Chem. A*, 2020, **8**, 19254-19261.

16. L.-A. Stern, L. Feng, F. Song and X. Hu, *Energy Environ. Sci.*, 2015, **8**, 2347-2351.

17. B. Qiu, A. Han, D. Jiang, T. Wang and P. Du, *ACS Sustain. Chem. Eng.*, 2019, **7**, 2360-2369.

18. Y. Yang, H. Fei, G. Ruan and J. M. Tour, *Adv. Mater.*, 2015, **27**, 3175-3180.

19. S. Chakrabartty, S. Karmakar and C. R. Raj, *ACS Appl. Nano Mater.*, 2020, **3**, 11326-11334.

20. F. Wang, J. Chen, X. Qi, H. Yang, H. Jiang, Y. Deng and T. Liang, *Appl. Surf. Sci.*, 2019, **481**, 1403-1411.